Available online at www.sciencedirect.com

SCIENCE DIRECT®

Applied Surface Science 222 (2004) 263–268

applied surface science

www.elsevier.com/locate/apsusc

Annealing effects on the microstructure and photoluminescence properties of Ni-doped ZnO films

D.J. Qiu[a,*], H.Z. Wu[a,b], A.M. Feng[c], Y.F. Lao[b], N.B. Chen[a], T.N. Xu[a]

[a]*Department of Physics, Zhejiang University, Tian Mu Shan Road, Hangzhou 310028, PR China*

[b]*State Key Laboratory of Functional Materials for Informatics, Shanghai Institute of Microsystem and Information Technology, Chinese Academy of Sciences, Shanghai 200050, PR China*

[c]*College of Metrology Engineering, China Institute of Metrology, Hangzhou 310034, PR China*

Received 11 July 2003; received in revised form 17 August 2003; accepted 18 August 2003

Abstract

Ni-doped ZnO (ZnO:Ni) films were fabricated on Si(0 0 1) substrates by reactive electron beam evaporation at low substrate temperature. The as-grown films were then annealed in oxygen ambient at higher temperatures. X-ray diffraction (XRD) results indicated that 5 at.% Ni-doped samples are still of single phase with the ZnO-like wurtzite structure. Photoluminescence (PL) measurements of Ni-doped samples illustrated the UV-PL emission centered at about 384 nm, which is ascribed to the near-band-edge (NBE) emissions of ZnO-like band structures. The UV-PL intensity becomes stronger along with the increase of annealing temperatures and reaches a maximum magnitude after annealed at 450 °C. However, along with the further increase of annealing temperatures, UV-PL intensity diminishes again. The UV-PL intensity of 450 °C-annealed samples is 213 times stronger than that of as-grown (doped) samples, which may render potential applications in optoelectronic devices, such as UV luminescent devices.

© 2003 Elsevier B.V. All rights reserved.

PACS: 81.15.Jj; 68.55.-a; 78.20.-e

Keywords: Ni-doped ZnO films; Electron beam reactive deposition; Microstructure; Photoluminescence

1. Introduction

In recent years doped ZnO thin films have been the subject of much attention because of their potentials for important applications such as luminescent materials, [1] gas sensors, [2] heterojunction solar cells, [3] transparent conductors, [4] and the diluted magnetic semiconductors (DMS) for use as the materials of spintronics [5,6]. Unintentionally doped ZnO films usually present n-type conductors owing to their incorporated large amount of O vacancies in the films, and have poor stability in corrosive environments or even in the humid air ambient. The electrical and optical properties of such ZnO films are often altered by adsorption of O_2, CO_2, CH groups, and water. Therefore, crystalline ZnO films have been doped to enhance their properties with elements of the groups IA, such as Li, and IIIA or VA, such as Al, Ga, In, N, P, As, Sb, etc. [7–12]. It is known that unintentionally doped ZnO film is an n-type conductor, while p-type

* Corresponding author. Tel.: +86-571-88273600; fax: +86-571-88836565.
E-mail address: qdj@yeah.net (D.J. Qiu).

0169-4332/$ – see front matter © 2003 Elsevier B.V. All rights reserved.
doi:10.1016/j.apsusc.2003.08.015

ZnO materials can be realized by doping with N, As or Sb [10–12]. On the other hand, doping zinc oxide materials with transition metal elements of the group VIII, such as Fe, Co and Ni, can attain the diluted magnetic semiconductors. However, doping was usually not done with transition elements of the groups IB and IIB, probably due to the incompatibility in the electron affinity or in the ionic radii of such elements with that of Zn.

With the intention to find new luminescent and spin-electronic materials, we report in this letter the doping of ZnO films with nickel (Ni) by reactive electron beam evaporation technique at a low substrate temperature. The as-grown (doped) films were then annealed in oxygen ambient at higher temperatures. The annealing effects on the ensuing changes in morphological, structural, and optical properties of Ni-doped ZnO films have been studied. The studies show remarkable modifications of these properties through such annealing.

2. Experimental

Ni-doped ZnO (ZnO:Ni) films were grown in a reactive e-beam evaporation system [13]. Fine-polished Si(0 0 1) wafers were used as substrates. The pretreatment of Si(0 0 1) substrates was the same as described earlier [14]. The evaporation sources both for ZnO and Ni epitaxial layers are the sintered polycrystalline ZnO and Ni (both with the purity of 99.95%) target, respectively. Ni-doped ZnO films were realized by evaporating the ZnO and Ni target alternately at a substrate temperature of 230 °C. Before evaporation the background pressure in the reaction chamber was 3.0×10^{-3} Pa, then the high-purity oxygen gas was introduced into the chamber and the gas pressure was kept at 3.0×10^{-2} Pa. During depositions of ZnO and Ni epitaxial layers, the partial vapor pressure of ZnO and Ni was set at 2.0×10^{-2} and 0.5×10^{-2} Pa, respectively. The growth rate for ZnO and Ni was about 3.8 and 0.8 Å/s, which was calibrated by ex situ film thickness measurements using a TENCOR α-step 200 profiler. The film surface roughness was also surveyed with the α-step profiler. All of Ni-doped ZnO films presented in this work are composed of five Ni layers. Each of Ni layer is nominally 10 Å in thickness and is sandwiched between two ZnO layers, while each of ZnO layer is nominally 200 Å in thickness except the first layer of ZnO on Si(0 0 1) substrate with thickness of nominally 1140 Å. The as-grown ZnO:Ni films were then annealed in oxygen ambient at different temperatures, 350, 450, 550 and 650 °C. The duration of each annealing treatment is same, 1 h. Energy dispersive X-ray detection (EDX) measurements were carried out to characterize the ratio of Ni:Zn (at.%) in Ni-doped ZnO films. Z-AFM-II atomic force microscope, D/Max-IIIB X-ray diffractometer, S-4700 II field emission scanning electron microscopy and Shimadzu RF-540 fluorophotometer were employed to characterize the plan and cross-sectional morphologies, microstructures and photoluminescent properties of ZnO:Ni films. In the PL measurements an ozone-free xenon lamp is used as the excitation source, the excitation line is set at 240 nm and the slit width of fluorophotometer is set at 10 nm. The detection energy is scanned from 330 to 650 nm and a filter is used to eliminate the disturbance of excitation source at 480 nm.

3. Results and discussion

A Comparison of AFM images of undoped and Ni-doped ZnO (ZnO:Ni) films grown on Si(0 0 1) substrates is shown in Fig. 1, (a) is for as-grown undoped ZnO, (b) is for as-grown ZnO:Ni film with an EDX measured Ni:Zn ratio of 5:95 at.% and, (c) is for the same ZnO:Ni film but has undergone annealing treatment at 650 °C for 1 h. The film thickness corresponding to Fig. 1a and b is 350 and 220 nm, respectively. By comparison of Fig. 1a and b, it is found that the surface morphologies of the two films are presumably same, i.e., both of the undoped and Ni-doped ZnO films present pillar-like growth characteristics. The strong resemblance of the surface morphologies between these two films is ascribed to the small concentration of Ni (5 at.%) in the doped film and the compatibility of ion radii between Ni^{2+} and Zn^{2+} [15]. Consequently, the average surface roughness of undoped and Ni-doped ZnO films are small, 4.8 and 3.5 nm, respectively. It is noted that the average surface roughness of Ni-doped ZnO film (3.5 nm) is slightly smaller than that of undoped ZnO film (4.8 nm), which is probably ascribed to their

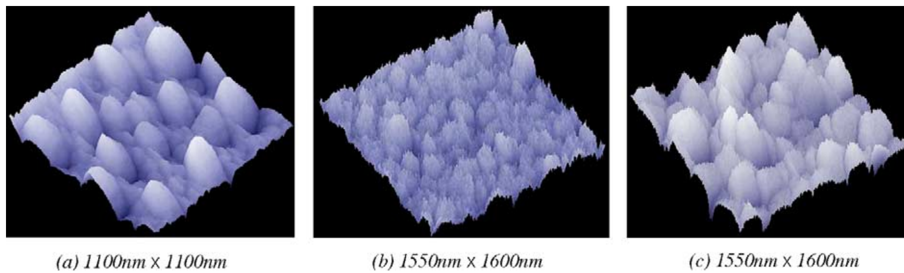

Fig. 1. Comparison of AFM images of undoped and 5 at.% Ni-doped ZnO (ZnO:Ni) films: (a) as-grown undoped ZnO, (b) as-grown ZnO:Ni and (c) 650 °C-annealed ZnO:Ni film.

discrepancy in thickness. On the other hand, by comparing the morphologies between the as-grown and annealed (at 650 °C) ZnO:Ni films shown in Fig. 1, it is found that although the annealed sample still presents pillar-like characteristics, its grain size turns much larger and its surface turns rougher.

The ratio of Ni and Zn in the doped film is investigated by the EDX measurement under the plan detection mode. The EDX spectroscopy is equipped on an S-570 scanning electron microscope (SEM). The size of focused electron spot in EDX experiment is about 2 μm in diameter and the spot is scanned within a selected area (60 μm × 40 μm) on the film. The penetrated depth of focused high energy electrons into the ZnO:Ni sample is about 2.5 μm. Fig. 2 illustrates the EDX pattern of an as-grown ZnO:Ni sample. As is seen, the peak at 7.47 keV is from radiation of Ni. The average Ni content in ZnO:Ni film is calculated according to the integral intensity of Ni peak with its ionization cross-section taken into account. The Ni:Zn ratio surveyed is 5:95 (at.%) with an experimental error of about 10% on account of the small thickness of ZnO:Ni film compared with the penetrated depth of focused high energy electrons in the EDX measurement.

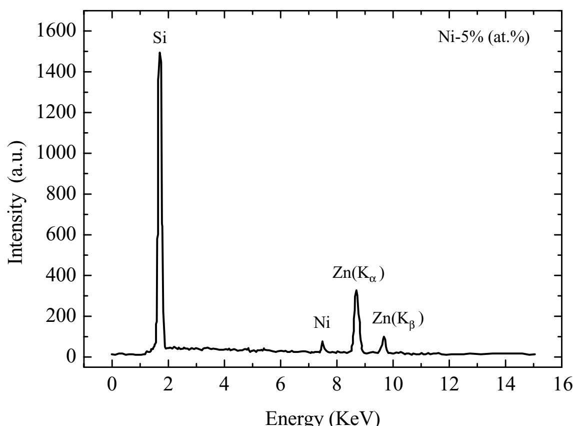

Fig. 2. An EDX pattern of Ni-doped ZnO film on Si(0 0 1). The ratio of Ni:Zn is 5:95 (at.%).

Fig. 3 shows the comparison of X-ray diffraction (XRD) patterns of as-grown ZnO:Ni films with different Ni contents. The ratio Ni:Zn for curves (a), (b) and (c) related samples are 5:95, 11:89 and 38:62 (at.%), respectively. As is seen, 5 at.% Ni-doped ZnO film is still of single phase with the highly *c*-axis oriented ZnO-like wurtzite structure, while other orientations such as (1 0 0) and (1 0 1) planes of ZnO-like structure and even with a Ni phase would emerge in XRD pattern if Ni content in ZnO:Ni film exceeding a certain concentration, as evidenced in curves (b) and (c) in Fig. 3. The line width of (0 0 2) diffraction peak for curve (a) is 0.32°, which is comparable to that of undoped ZnO film grown on Si(0 0 1) substrate (0.28°) [14], indicating its good crystallite quality. The *c*-axis oriented single phase property of 5 at.% Ni-doped ZnO is possibly due to its small Ni content and to that Ni residues in the film incorporated into the lattice of ZnO crystallites as interstitial or substitutional impurities. Ni substitutional impurities would be formed by Ni^{2+} ions partly substituting the Zn^{2+} sites in the lattice, because Ni^{2+} ions are prone to be formed in the oxygen environment. On the other hand, for the 5 at.% Ni-doped ZnO sample it is found that after annealed at appropriate temperature the line width of its (0 0 2) diffraction peak turns narrower compared with that of as-grown ZnO:Ni. The line width of 350 °C-annealed sample is narrower than that of as-grown film, and the line width of 450 °C-annealed sample is even narrower than that

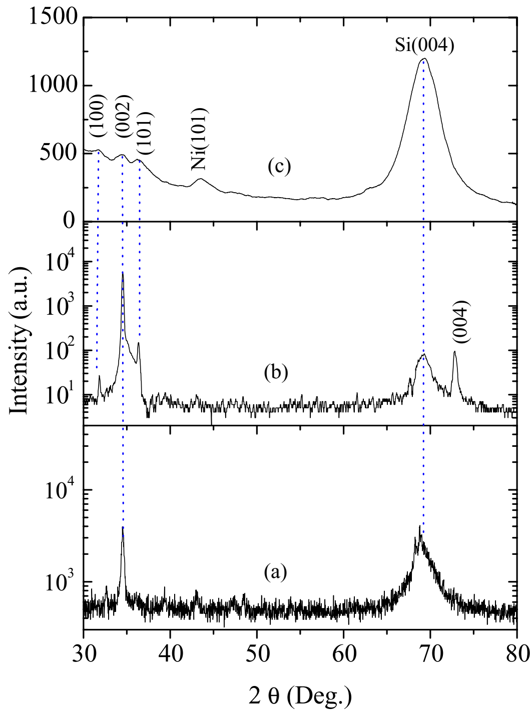

Fig. 3. Comparison of XRD patterns of as-grown ZnO:Ni films with different Ni contents. The ratio Ni:Zn for curves (a), (b) and (c) related samples are 5:95, 11:89 and 38:62 at.%, respectively.

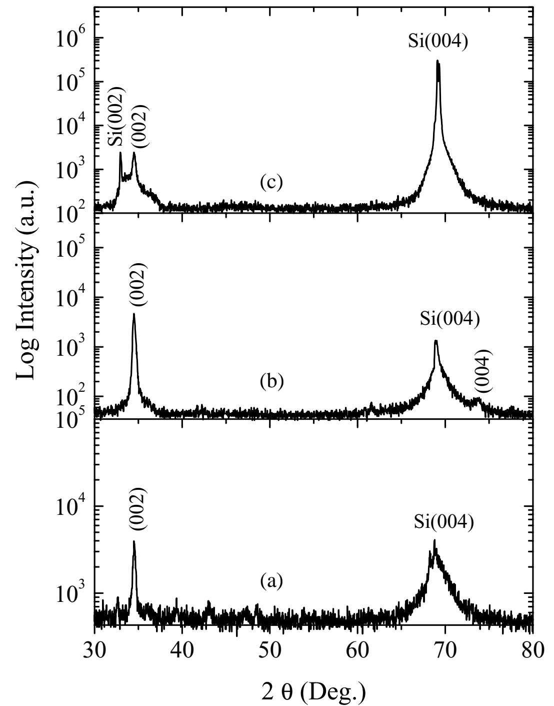

Fig. 4. Comparison of XRD patterns of 5 at.% Ni-doped ZnO sample as-grown and annealed at different temperatures: (a) as-grown, (b) 450 °C-annealed and (c) 650 °C-annealed.

of 350 °C-annealed one. Shown in Fig. 4 is the comparison of XRD patterns of 5 at.% Ni-doped ZnO samples as-grown and annealed at different temperatures. Curve (a) in Fig. 4 is for as-grown ZnO:Ni film and (b) is related to 450 °C-annealed sample, whose FWHM of dominant (0 0 2) diffraction peak is 0.26°, which is 0.06° narrower than that of as-deposited sample (0.32°). The narrower line width of (0 0 2) peak of 450 °C-annealed sample suggests its better crystal quality. The crystal quality improvement of ZnO:Ni film after annealed at 450 °C is mainly attributed to the recovery of microstructural defects and the homogenization of the film. However, along with the further increase in the annealing temperatures, such as at 550 or 650 °C, the crystallite quality of ZnO:Ni films deteriorated. As seen from curve (c) of 650 °C-annealed sample in Fig. 4 that, besides the (0 0 2) peak which is from the ZnO-like wurtzite structure of the film, a substrate peak of Si(0 0 2) and a broad amorphous phase are also emerged in the region from 32 to 37°, indicating the deterioration of the lattice and the degradation of the film quality because the high annealing temperature (such as 650 °C) caused the desorption of oxygen in the ZnO lattice. It is interestingly found the modifications in XRD patterns with different annealing temperatures are in good agreement with the changes in luminescent properties that will be discussed in the following section.

Shown in Fig. 5 is a high-resolution cross-sectional FESEM image of the as-grown ZnO:Ni film with Ni content of 5 at.%. It is noted that the high-brightened strip with thickness of about 30 nm is the SiO_2 layer. The SiO_2 layer was formed prior to the deposition of the first ZnO layer owing to the oxygen-enriched growth environment. On the other hand, as seen from Fig. 5 that the epitaxial film thickness is 210 nm which is consistent with our design that the total thickness of the multilayer ZnO:Ni film is about 220 nm. However, the prominent characteristics of the cross-sectional FESEM image is that only three interfaces, Si/SiO_2, SiO_2/ZnO and ZnO/ZnO:Ni, are clearly seen, while the

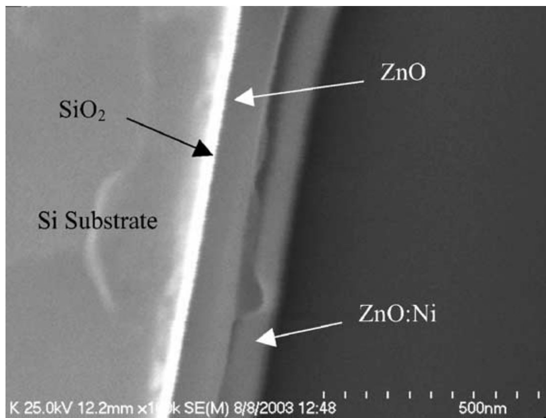

Fig. 5. High resolution cross-sectional FESEM image of as-grown ZnO:Ni film with Ni content of 5 at.%.

interfaces between Ni and ZnO layers are illegible. The illegibility of Ni/ZnO interfaces is probably attributed to the fact that the Ni layers are ultrathin (about 10 Å) and to the diffusion interactions between Ni and ZnO layers. Consequently, the slightly (5 at.%) Ni-doped multilayer ZnO:Ni film, even achieved at a relatively low growth temperature (230 °C), presents its quasi-homogenization of compositional distribution along the *c*-axis direction perpendicular to the substrate surface and only the main interfaces, Si/SiO_2, SiO_2/ZnO and ZnO/ZnO:Ni are observed.

Fig. 6 illustrates the comparisons of room temperature photoluminescence (PL) spectra between as-grown and annealed ZnO:Ni samples with Ni content of 5 at.%. It is seen that a peak centered at 384 nm dominates all of the PL spectra, which is ascribed to the near-band-edge (NBE) recombination transitions of ZnO-like band structures of Ni-doped ZnO films (the room temperature band gap of ZnO is about 3.37 eV). However, a prominent feature of the NBE emission is the asymmetry of the broad line shape. One can model each of the PL spectra as a superposition of two Gaussian lines centered at 384 and 470 nm, which are probably attributed to the emissions from free excitons of ZnO-like electronic structures and from Ni^{3+} and/or interstitial oxygen related impurities, respectively [16]. On the other hand, it is found the PL intensity becomes stronger along with the increase of annealing temperatures and reaches a maximum magnitude after annealed at 450 °C. Shown

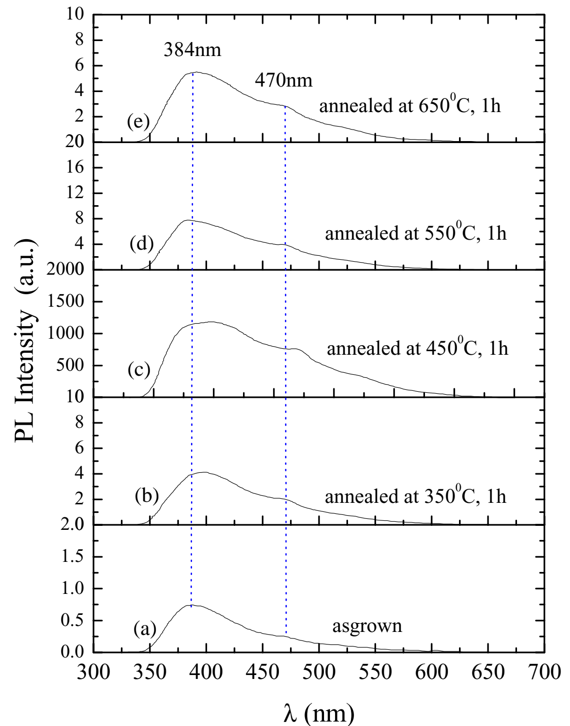

Fig. 6. Comparisons of UV-PL properties of 5 at.% Ni-doped ZnO (ZnO:Ni) film as-grown and annealed at different temperatures: (a) as-grown, (b) 350 °C-annealed, (c) 450 °C-annealed, (d) 550 °C-annealed and (e) 650 °C-annealed.

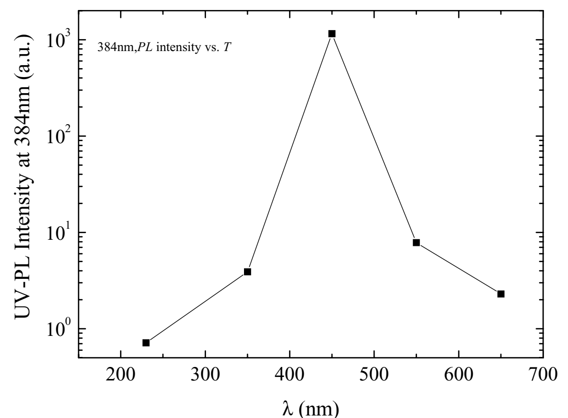

Fig. 7. UV-PL intensities at 384 nm as a function of annealing temperatures.

in Fig. 7 is UV-PL intensities at 384 nm as a function of annealing temperatures. As is seen, the UV-PL peak intensity of 450 °C-annealed samples is 213 times stronger than that of as-grown (doped) samples. The mechanism of UV-PL intensity enhancement along with the increase of annealing temperature is the recovery of microstructural defects and the homogenization of the film, just as what has been verified by XRD measurements as shown in Fig. 4b. However, along with the further increase in the annealing temperatures, such as annealed at 550 or 650 °C, the UV-PL intensity of ZnO:Ni films decreased again, suggesting the deterioration of the lattice and degrading of the film because of the too high annealing temperatures. The annealing temperature dependent PL properties of 5 at.% Ni-doped ZnO films are well consistent with their XRD results. And the ultrahigh UV-PL intensities of such ZnO:Ni films after annealed at appropriate temperature (about 450 °C) would make them very important in applications such as UV luminescent materials.

4. Conclusions

In conclusion, Ni-doped ZnO (ZnO:Ni) films with different nickel content were achieved on Si(0 0 1) substrates by reactive electron beam evaporation at low substrate temperature. XRD results indicated that slightly Ni-doped (5 at.%) samples are still of single phase with the highly *c*-axis oriented ZnO-like wurtzite structure. Annealing ZnO:Ni films at appropriate temperatures would result in the recovery of microstructural defects and the homogenization of the film, and consequently, enhance the UV-PL intensities of ZnO:Ni films by more than two orders of magnitude. The ultrahigh UV-PL intensities of appropriate temperature annealed ZnO:Ni films would make them very important in applications such as UV luminescent materials.

Acknowledgements

This work is supported by the National Natural Science Foundation of China under Grant No. 10174064, and Natural Science Fund of Zhejiang Province.

References

[1] A. Miyake, H. Kominami, H. Tatsuoka, H. Kuwabara, Y. Nakanishi, Y. Hatanaka, J. Cryst. Growth 214–215 (2000) 294.
[2] V. Nigel, V. Alan, W. Alan, Nuclear Instrum. Methods Phys. Res. B 97 (1995) 575.
[3] D. Song, A.G. Aberle, J. Xia, Appl. Surf. Sci. 195 (2002) 291.
[4] M.A. Martinez, J. Herrero, M.T. Gutierrez, Solar Energy Mater. Solar Cells 45 (1997) 75.
[5] K. Ueda, H. Tabata, T. Kawai, Appl. Phys. Lett. 79 (2001) 988.
[6] H. Katayama, K. Sato, Physica B 327 (2003) 337.
[7] R.J. Hong, X. Jiang, B. Szyszka, V. Sittinger, A. Pflug, Appl. Surf. Sci. 207 (2003) 341.
[8] K. Haga, P.S. Wijesena, H. Watanabe, Appl. Surf. Sci. 169–170 (2001) 504.
[9] G.K. Paul, S.K. Sen, Mater. Lett. 57 (2002) 742.
[10] Y.G. Wang, S.P. Lau, X.H. Zhang, H.W. Lee, H.H. Hng, B.K. Tay, J. Cryst. Growth 252 (2003) 265.
[11] X.L. Guo, H. Tabata, T. Kawai, J. Cryst. Growth 223 (2001) 135.
[12] Y.R. Ryu, S. Zhu, D.C. Look, J.M. Wrobel, H.M. Jeong, H.W. White, J. Cryst. Growth 216 (2000) 330.
[13] H.Z. Wu, D.J. Qiu, Y.J. Cai, X.L. Xu, N.B. Chen, J. Cryst. Growth 245 (2002) 50.
[14] D.J. Qiu, H.Z. Wu, X.L. Xu, N.B. Chen, Chin. Phys. Lett. 19 (2002) 1714.
[15] A.E. Jiménez-González, J. Solid State Chem. 128 (1997) 176.
[16] A. Šurca, B. Orel, B. Pihlar, P. Bukovec, J. Electroanal. Chem. 408 (1996) 83.